ChemComm

COMMUNICATION

View Article Online
View Journal | View Issue

Cite this: *Chem. Commun.*, 2018, **54**, 12642

Received 14th September 2018,
Accepted 18th October 2018

DOI: 10.1039/c8cc07475e

rsc.li/chemcomm

Self-assembled adhesive biomaterials formed by a genetically designed fusion protein†

Pulakesh Aich,‡[a] Jaeyeon An,‡[b] Byeongseon Yang,‡[c] Young Ho Ko,[a] Junghyun Kim,[a] James Murray,[a] Hyung Joon Cha,*[c] Joon Ho Roh,*[a] Kyeng Min Park*[a] and Kimoon Kim*[ab]

Here we report a recombinant protein (MS) obtained by genetic fusion of a mussel foot protein (Mfp3) motif into a silk spidroin (MaSp1). The MS not only self-assembled into a supramolecular fibre, as does the parent MaSp1, but also showed enhanced adhesiveness resulting from the DOPA-containing Mfp3 portion. The successful incorporation of the wet adhesiveness of Mfp3 into the well-structured assembly of MaSp1 may provide a new insight for the genetic design of underwater adhesive recombinant proteins by utilizing the structural features of a spidroin protein.

Nature exhibits many biomaterials with remarkable chemical and physical properties that often inspire researchers to develop new functional materials. For example, tough biomimetic fibres inspired by spider silk draglines have outstanding mechanical properties;[1,2] such properties are attributed to their well-defined tertiary structure which is self-assembled from major ampullate spidroin 1 (MaSp1, accounting for the crystalline fraction of spider webs).[3,4] The large proportion of nonpolar and hydrophobic amino acids such as glycine and alanine plays a crucial role in forming a β-sheet structure by providing robust inter- and intra-molecular interactions. The assembly uses its good elastic properties to maintain its structure; it achieves this by releasing applied stress through stick-slip deformation of the protein assemblies.[5] To capture prey in its web, natural spider silks are not only mechanically robust and flexible but also adhesive. The combined properties are a result of the hierarchical organization of various silk proteins including silk dragline, spiral and glue proteins.[6] Development of biomaterials with such a collection of properties is extremely challenging.

Mussel foot proteins (Mfp1, 2, 3, 4, 5 and 6) present in the surface adhered flatten plaques of mussel byssus have been extensively studied to understand their remarkable underwater adhesion properties.[7,8] Among these, Mfp3 and Mfp5 have been found to be important proteins for underwater interfacial adhesion because of their relatively large proportion (20–30 mol% in the proteins) of L-3,4-dihydroxyphenylalanine (DOPA) compared to that of other Mfps.[9] Numerous studies revealed that DOPA is an important chemical moiety in Mfps for underwater adhesion to various organic/inorganic surfaces. Until now, the reported roles of DOPA include the dehydration of a wet surface, and adhesion to the surface through various interactions including hydrogen bonding, metal oxide coordination and cation–π interactions.[10] To take advantage of this interesting behaviour, DOPA has been chemically conjugated to polymers, nanoclays and metal nanoparticles as well as enzymatically transformed on proteins from tyrosine, and exploited as a crosslinker and adhesive to develop various soft-materials including adhesive hydrogels, actuators and self-healing materials.[11–18] Although these materials showed the great potential of Mfps as adhesive biomaterials, the adhesion property of the materials was not as good as that of the natural Mfps which are hierarchically organized with other biomolecules in plagues. Since the adhesion property was significantly influenced by the structural order of the materials,[19] a rational design of bioadhesives which complements a well-ordered structure to adhesive Mfps is highly required to enhance the adhesion ability.

Using a genetic engineering, herein, we demonstrate a successful genetic fusion of Mfp3 (from *Mytilus galloprovincialis*)[20] showing adhesiveness to MaSp1 (from *Nephila clavipes*)[21] self-assembled into a well-defined supramolecular structure to develop a new type of recombinant protein-based adhesive biomaterials (Fig. 1). The structural characteristics of the newly designed recombinant protein (MS) resembled those of MaSp1; namely, they formed fibres. Furthermore, it showed enhanced adhesiveness in a wet condition compared to that of MaSp1, which suggests the great

[a] *Center for Self-assembly and Complexity, Institute for Basic Science (IBS), Pohang, 37673, Republic of Korea. E-mail: jhroh@ibs.re.kr, kmpark@ibs.re.kr, kkim@postech.ac.kr; Web: http://csc.ibs.re.kr*

[b] *Department of Chemistry, Pohang University of Science and Technology, Pohang, 37673, Republic of Korea*

[c] *Department of Chemical Engineering, Pohang University of Science and Technology, Pohang, Korea. E-mail: hjcha@postech.ac.kr; Web: http://magic.postech.ac.kr*

† Electronic supplementary information (ESI) available: Supplementary figures and table, experimental procedures. See DOI: 10.1039/c8cc07475e

‡ These authors contributed equally to this work.

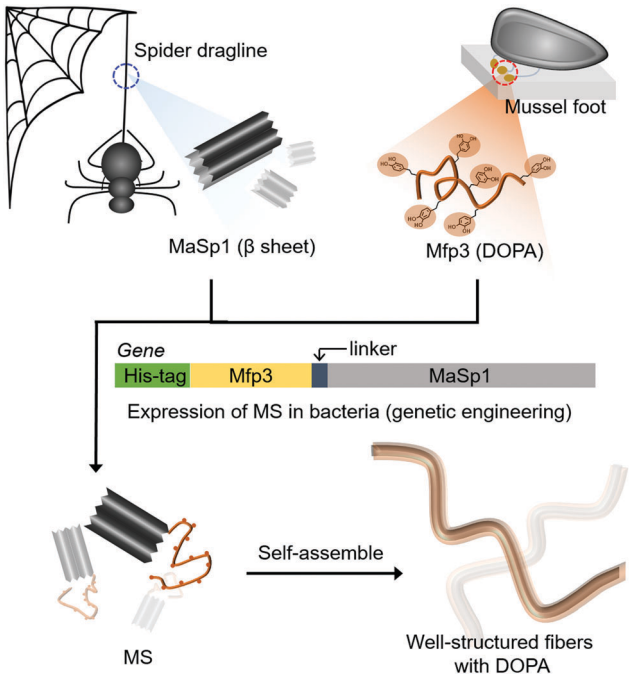

Fig. 1 Schematic illustration of genetic fusion of Mfp3 into MaSp1 and their self-assembly to form DOPA containing supramolecular fibres.

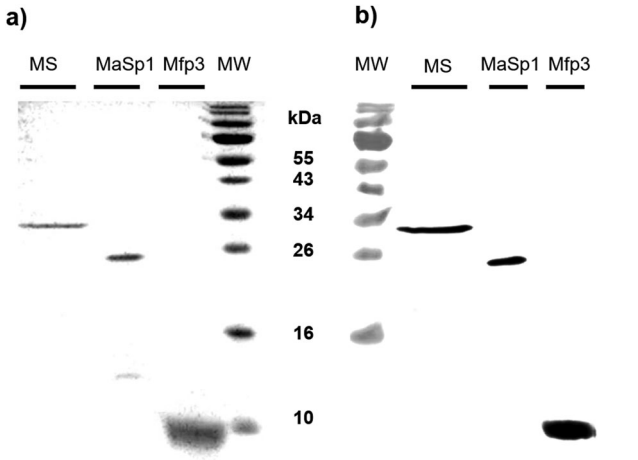

Fig. 2 (a) SDS-PAGE gel of the purified recombinant proteins stained with Coomassie brilliant blue and (b) western blotting of (a) with anti His-tag primary antibody which was visualized by HRP conjugated-secondary antibody.

potential of this new genetic design for recombinant proteins as advanced bio-adhesives.

For expression of the recombinant protein (27.9 kDa), plasmid DNA containing Mfp3 (6.8 kDa) and MaSp1 (22.0 kDa) was used; the proteins were connected by a flexible glycine-serine linker "GGGGS" for enhanced functionally active protein expression.[22] Hexa-histidine tag (His-tag) was inserted at the N-terminus of the recombinant protein for immobilized metal affinity chromatography (IMAC) purification[23] (Table S1 for the individual sequence for the proteins, see the ESI†). The target protein in a lysate of the bacteria was anchored to Ni-nitrilotriacetic acid (Ni-NTA) resins having His-tag binding affinity. Since DOPA is a non-canonical amino acid, the protein anchored to the resin was treated with an enzyme (tyrosinase) for transformation of tyrosine to DOPA.[24,25] After His-tag affinity chromatography, the purified protein was analysed by SDS-PAGE gel (See the ESI† for synthesis and purification). The protein band stained with Coomassie brilliant blue appeared at 28 kDa (Fig. 2a), which agreed well with sum of molecular weight of Mfp3 (6.8 kDa) and MaSp1 (22.0 kDa). The mass of the protein was confirmed by a molecular ion peak at 27.9 kDa (Fig. S1a, see the ESI†) in matrix assisted laser desorption and ionization time of flight mass spectroscopy (MALDI-ToF MS). In addition, the detection of the purified proteins in a western blot assay by anti His-tag primary antibody with horseradish peroxidase (HRP)-conjugated secondary antibody (Fig. 2b) confirmed the successful expression and purification of the target recombinant protein, MS.

To validate the incorporation of DOPA into MS, we performed a nitroblue tetrazolium (NBT) assay (see the ESI†).[26] This assay quantifies the amount of DOPA in the protein by detecting increase of absorption at 530 nm, which is a measure of formation of the blue-coloured diformazan from NBT upon oxidation of DOPA in a solution of NBT/K-glycinate. In the NBT assay with MS, we observed a blue-coloured band when blotted the protein solution on a nitrocellulose membrane, indicating that MS has DOPA converted from tyrosine (Fig. S2, see the ESI†). The quantitative analysis of the UV-Visible absorption revealed that *ca.* 3.2 tyrosine residues out of 16 (20%) had been converted to DOPA in MS. In addition, MALDI-ToF MS analysis showed 50 Da higher molecular ion peak of MS after treating with tyrosinase compared to that of MS before treating (Fig. S1c, see the ESI†). It supported transformation of *ca.* 3.1 DOPA from tyrosine residues which is well-matched with that from UV-Vis. The structure of MS was analysed by circular dichroism (CD) and SEM. CD spectra of Mfp3, MaSp1 and MS revealed that the shape of the spectrum of MS is different from that of Mfp3, but highly similar to that of MaSp1 (Fig. 3a). These CD spectra suggested that the MaSp1 portion in MS governed the final structure of the protein assembly. To visualize the structure, we performed SEM of the proteins after lyophilisation (see the ESI†). The SEM images of these proteins showed that MS formed fibres (diameter = 770 ± 90 nm, Fig. 2b) similar to those of MaSp1 (diameter = 750 ± 40 nm, Fig. 2d) whereas Mfp3 did not form such fibres (Fig. 2c). In addition, MS with tyrosine before transformed into DOPA also showed a similar fibre formation with MaSp1 in SEM (Fig. S3, see the ESI†). These results also strongly suggested that the MaSp1 portion played a crucial role in forming such a hierarchical supramolecular structure of the recombinant protein, MS. MaSp1 and Mfp3 in MS seemed to act as a rigid and flexible segment, respectively, in the protein to self-assemble into a fibre, similar to those in synthetic macromolecules forming unique self-assembled structures with functions.[27–29]

To study the influence of the hierarchical structure of MS on its elasticity, we performed dynamic mechanical analysis of MS (see the ESI†). MS (10 μL, 2.5 nmol) was loaded in between two circular mica surfaces before the measurement (see the ESI†).

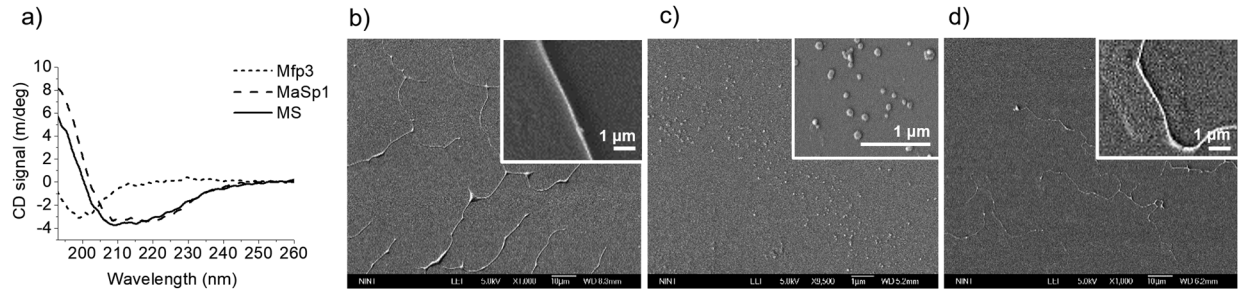

Fig. 3 (a) CD spectra of MS (solid line), Mfp3 (small dashed line) and MaSp1 (large dashed line), and SEM images of (b) MS, (c) Mfp3 and (d) MaSp1.

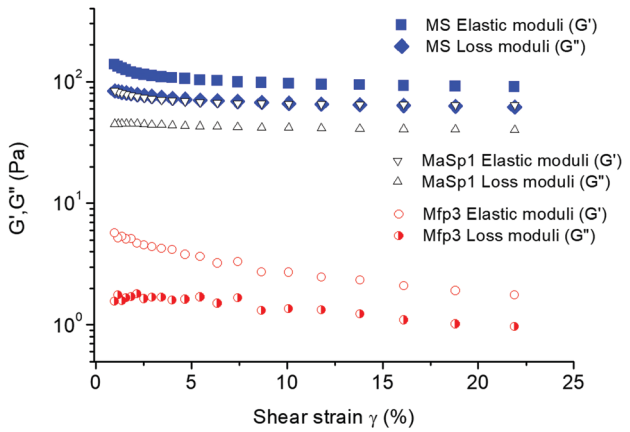

Fig. 4 Dynamic mechanical analysis of MS, MaSp1 and Mfp3 using a rheometer. Shear strain dependent elastic modulus (G') and loss modulus (G'') at constant frequency sweep (10 rad s^{-1}).

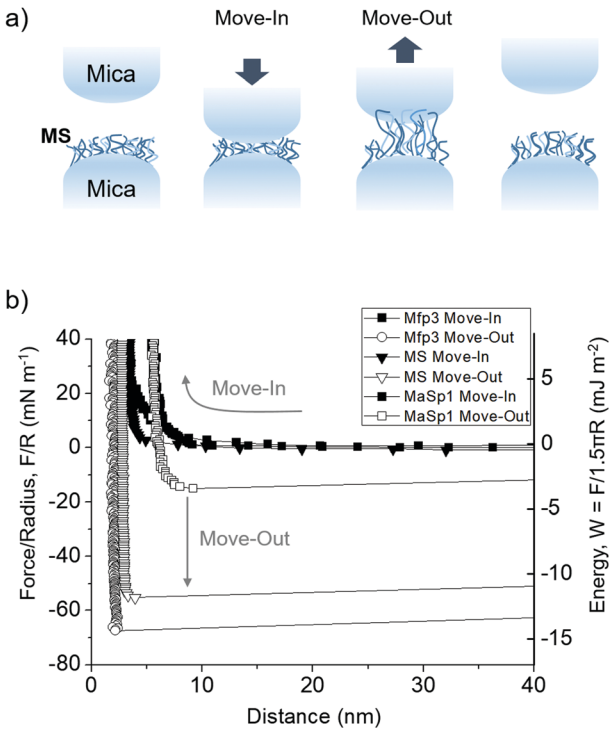

Fig. 5 (a) Schematic illustration of SFA analysis of surface adhesion interactions and (b) the result of SFA measurement for Mfp3, MaSp1 and MS. The normalized forces (F/R) and its corresponding interaction energies per unit area (defined as $F/1.5\pi R$) are shown on the left and right ordinates, respectively.

The MS was found to have a typical viscoelastic soft material behaviour showing non-linear shear strain-dependent loss of elastic modulus (G') which was also higher than the loss modulus (G'') over the whole range of the shear strain (Fig. 4). Comparison of the modulus values (G' and G'') for Mfp3 and MaSp1, measured in the same condition as above (Fig. 4), revealed that MaSp1 had at least 10-fold higher elastic moduli than Mfp3. This result clearly supported that MS formed well-organized fibres making it significantly more elastic than Mfp3. The elasticity of MS is closer to that of MaSp1 than it is to Mfp3, suggesting that the elasticity of MS seemed to be originated from the MaSp1 motif of MS. A close comparison of MS and MaSp1 revealed that MS was *ca.* 2 times more elastic than MaSp1. This result indicated that the genetic fusion of Mfp3 reinforced elasticity of the self-assembled structure of MS. The enhanced elasticity *via* the long-range self-assembly into fibres reduces failure not only in cohesion but also in adhesion across the adhesive/surface interface because they are better able to dissipate energy through their flexible structure.

After the structural and the dynamic mechanical analysis of the recombinant protein-based supramolecular structures, we investigated the surface adhesiveness of MS to mica in a wet condition. The interaction force between MS and mica was measured using Surface Force Apparatus (SFA) as per the literature report[30] (see the ESI†). One mica surface was treated with a sufficient amount of the protein to cover the whole surface, then washed and contacted to the other mica surface for 10 min (Fig. 5a). The normalized force (force/radius, F/R) to detach MS from mica was measured to be 55 mN m^{-1} (Fig. 5b), which was converted to 12 mJ m^{-2} as surface adhesion energy per unit area (W) by following the equation, $W = F/1.5\pi R$, as reported earlier.[30] We also performed the same experiment as above with MaSp1, instead of MS, to directly compare the surface adhesion energy between them. This measurement revealed that MaSp1 also showed adhesion ability with the energy of 4 mJ m^{-2} (Fig. 5b) which is 3-fold lower than that of MS. This result clearly indicated that MS showed significantly enhanced surface adhesion ability compared to MaSp1 which does not contain a DOPA moiety in the SFA measurement. When compared to the SFA result of Mfp3 (14 mJ m^{-2}), MS showed 1.2-fold less adhesion energy. At a glance, this result seemed to indicate that MS did not provide enhanced surface adhesion property compared to Mfp3. However, considering the density of the MS molecules on the

surface in the SFA measurements estimated based on the hydrodynamic radii of the proteins (1.9 nm and 3.3 nm for Mfp3 and MS, respectively), measured by diffusion-ordered spectroscopy (DOSY) in D_2O (Fig. S4, see ESI† for detail), the number of MS molecules can be 2.9-fold fewer than that of Mfp3. The adhesion energy per protein molecule of MS is 2.5-fold greater than that of Mfp3. In other words, one protein molecule of MS can be 2.5-fold more adhesive than that of Mfp3.

Taken together, a recombinant protein of MS containing Mfp3 and MaSp1 motifs showed significantly enhanced adhesiveness compared to MaSp1 alone. Such enhanced underwater adhesiveness of MS seems to be due to the molecular basis of the recombinant protein. Specifically, the genetic fusion of Mfp3 into MaSp1 yields more elastic and underwater sticky self-assembled fibres with presentation of DOPA moieties. Higher elasticity induced by the formation of supramolecular structures probably plays a central role in alleviating both cohesive and adhesive stress of MS by better dissipating energy across protein molecules.

In summary, we demonstrated a recombinant protein-based bio-adhesive by inserting one natural protein into another, namely Mfp3 into MaSp1. The resulting spidroin-based protein forming an elastic fibril structure showed underwater adhesiveness because of the mussel foot protein motif. The enhanced properties were confirmed by dynamic mechanical analysis with a rheometer and underwater adhesion measurement by SFA. In principle, the number of DOPA moieties in the protein can be increased by enhancing the conversion of DOPA from tyrosine in the protein with adopting longer glycine-serine linkers in genetic design or *in vivo* residue-specific incorporation of DOPA using misaminoacylation;[31] thus the adhesiveness of the biomaterials can be further improved. This study may provide new insights for the design of underwater adhesive recombinant proteins based on the structural features of a spidroin protein, which can be potentially useful for various bioapplications including biomedical uses such as glues for soft tissues.

This work was supported by the Institute for Basic Science (IBS) [IBS-R007-D1] (to K. K.) and Marine Biotechnology Program of the Korea Institute of Marine Science and Technology Promotion funded by the Ministry of Oceans and Fisheries (to H. J. C.).

Conflicts of interest

There are no conflicts to declare.

Notes and references

1 M. Xu and R. V. Lewis, *Proc. Natl. Acad. Sci. U. S. A.*, 1990, **87**, 7120–7124.
2 F. Vollrath, *J. Biotechnol.*, 2000, **74**, 67–83.
3 L. Romer and T. Scheibel, *Prion*, 2008, **2**, 154–161.
4 X. Hu, K. Vasanthavada, K. Kohler, S. McNary, A. M. Moore and C. A. Vierra, *Cell. Mol. Life Sci.*, 2006, **63**, 1986–1999.
5 S. W. Cranford, A. Tarakanova, N. M. Pugno and M. J. Buehler, *Nature*, 2012, **482**, 72–76.
6 T. Scheibel, *Microb. Cell Fact.*, 2004, **3**, 14.
7 B. P. Lee, P. B. Messersmith, J. N. Israelachvili and J. H. Waite, *Annu. Rev. Mater. Res.*, 2011, **41**, 99–132.
8 A. H. Hofman, I. A. van Hees, J. Yang and M. Kamperman, *Adv. Mater.*, 2018, **30**, 1704640.
9 Q. Lin, D. Gourdon, C. Sun, N. Holten-Andersen, T. H. Anderson, J. H. Waite and J. N. Israelachvili, *Proc. Natl. Acad. Sci. U. S. A.*, 2007, **104**, 3782–3786.
10 G. P. Maier, M. V. Rapp, J. H. Waite, J. N. Israelachvili and A. Butler, *Science*, 2015, **349**, 628–632.
11 M. R. Kim and T. G. Park, *J. Controlled Release*, 2002, **80**, 69–77.
12 M. Brodie, L. Vollenweider, J. L. Murphy, F. Xu, A. Lyman, W. D. Lew and B. P. Lee, *Biomed. Mater.*, 2011, **6**, 015014.
13 A. K. Gaharwar, S. A. Dammu, J. M. Canter, C. J. Wu and G. Schmidt, *Biomacromolecules*, 2011, **12**, 1641–1650.
14 B. P. Lee and S. Konst, *Adv. Mater.*, 2014, **26**, 3415–3419.
15 B. K. Ahn, D. W. Lee, J. N. Israelachvili and J. H. Waite, *Nat. Mater.*, 2014, **13**, 867–872.
16 L. Han, X. Lu, K. Liu, K. Wang, L. Fang, L. T. Weng, H. Zhang, Y. Tang, F. Ren, C. Zhao, G. Sun, R. Liang and Z. Li, *ACS Nano*, 2017, **11**, 2561–2574.
17 Q. Zhu and Q. Pan, *ACS Nano*, 2014, **8**, 1402–1409.
18 J. Horsch, P. Wilke, M. Pretzler, M. Seuss, I. Melnyk, D. Remmler, A. Fery, A. Rompel and H. G. Borner, *Angew. Chem., Int. Ed.*, 2018, DOI: 10.1002/anie.201809587.
19 R. J. Stewart, T. C. Ransom and V. Hlady, *J. Polym. Sci., Part B: Polym. Phys.*, 2011, **49**, 757–771.
20 S. C. Warner and J. H. Waite, *Mar. Biol.*, 1999, **134**, 729–734.
21 O. Tokareva, M. Jacobsen, M. Buehler, J. Wong and D. L. Kaplan, *Acta Biomater.*, 2014, **10**, 1612–1626.
22 R. Trinh, B. Gurbaxani, S. L. Morrison and M. Seyfzadeh, *Mol. Immunol.*, 2004, **40**, 717–722.
23 P. N. Hengen, *Trends Biochem. Sci.*, 1995, **20**, 285–286.
24 C. Zhong, T. Gurry, A. A. Cheng, J. Downey, Z. T. Deng, C. M. Stultz and T. K. Lu, *Nat. Nanotechnol.*, 2014, **9**, 858–866.
25 M. J. C. Long and L. Hedstrom, *ChemBioChem*, 2012, **13**, 1818–1825.
26 P. B. Issopoulos, *Pharm. Weekbl.*, 1989, **11**, 213–217.
27 Y. Kim, W. Li, S. Shin and M. Lee, *Acc. Chem. Res.*, 2013, **46**, 2888–2897.
28 Z. Huang, S. K. Kang, M. Banno, T. Yamaguchi, D. Lee, C. Seok, E. Yashima and M. Lee, *Science*, 2012, **337**, 1521–1526.
29 B. Sun, Y. Kim, Y. Q. Wang, H. X. Wang, J. Kim, X. Liu and M. Lee, *Nat. Mater.*, 2018, **17**, 599–604.
30 B. Yang, C. Lim, D. S. Hwang and H. J. Cha, *Chem. Mater.*, 2016, **28**, 7982–7989.
31 B. Yang, N. Ayyadurai, H. Yun, Y. S. Choi, B. H. Hwang, J. Huang, Q. Lu, H. Zeng and H. J. Cha, *Angew. Chem., Int. Ed.*, 2014, **53**, 13360–13364.